ORIGINAL ARTICLE

Apparent calibration shift of the Scintrex CG-5 gravimeter caused by reading-dependent scale factor and instrumental drift

Shin'ya Onizawa[1]

Abstract

Calibration measurements of the Scintrex CG-5 gravimeter were conducted using absolute gravity stations of the Japan Gravity Standardization Net, to constrain the scale factor and its temporal changes. The calibration data were obtained from a total gravity interval of 1.4 Gal through six campaigns, conducted for over 5 years between years 2012 and 2017. The scale factors varied by 1500 ppm in a range from 0.9991 to 1.0006, according to station combinations of the six campaigns. The scale factor depends primarily on the gravity reading ranges: for similar gravity reading ranges, no significant differences in the estimated scale factors were recognised, even though station combinations and observed times are different. Therefore, the gravity readings can be corrected by introducing a gravity reading-dependent scale factor. Furthermore, even though the scale factor essentially depends on gravity readings and not on time, temporal changes were observed during repeated calibration measurements at the same station combinations. A long-term instrumental drift of the CG-5 gravimeter could explain this phenomenon. In conclusion, the calibration shifts recognised during repeated measurements were apparently caused by: (1) the scale factor dependence on the gravity reading ranges and (2) the shift of the gravity reading ranges due to the instrumental drift.

Keywords Gravimeter · Scintrex CG-5 · Scale factor · Calibration shift · Instrumental drift

1 Introduction

Repeated microgravity surveys using relative gravimeters have been widely applied to monitor subsurface mass and/or density changes associated with volcanic activities, groundwater flows, exploitation of geothermal resources, and so on (e.g., Biegert et al. 2008; Williams-Jones et al. 2008). In microgravity measurements aimed at detecting gravity changes in the order of μGal ($1\,\text{Gal} = 10^{-2}\,\text{m/s}^2$), the sensitivity of instruments (i.e., the scale factor) should be properly calibrated according to target gravity intervals. If the scale factor is not well calibrated and the measurements include wide gravity intervals, there will be prominent discrepancies from the true relative gravity values. Furthermore, temporal changes in the scale factor, so-called calibration shifts, are reported for relative gravimeters like the LaCoste & Romberg model-G (Carbone and Rymer 1999), the Scintrex CG-3M

(Budetta and Carbone 1997; Ukawa et al. 2010) and the CG-5 (Parseliunas et al. 2011; Meurers 2018). Unless the scale factor and its temporal changes are calibrated, the observed gravity changes and any interpretation based on these data will be unreliable.

The Meteorological Research Institute, Japan Meteorological Agency (MRI), has been conducting microgravity surveys at active volcanoes such as Izu-Oshima since 2008, using the Scintrex CG-5 S/N: 300500033 (CG-5#033) gravimeter. However, the scale factor of the CG-5#033 has not been calibrated so far. In order to constrain the scale factor and its temporal changes of the CG-5#033 gravimeter, a series of calibration measurements have been conducted since 2012, using absolute gravity stations within a nationwide network: the Japan Gravity Standardization Net (JGSN; Fig. 1). The calibration measurements, performed over a period of 5 years and with a total gravity interval of 1.4 Gal, revealed important features about the scale factor of the CG-5#033 gravimeter.

The purpose of this study is to describe the occurrence of variations in the scale factor of the CG-5#033 gravimeter and illustrate a way to calibrate it. First, I describe the calibration

✉ Shin'ya Onizawa
  sonizawa@mri-jma.go.jp

[1] Meteorological Research Institute, Japan Meteorological
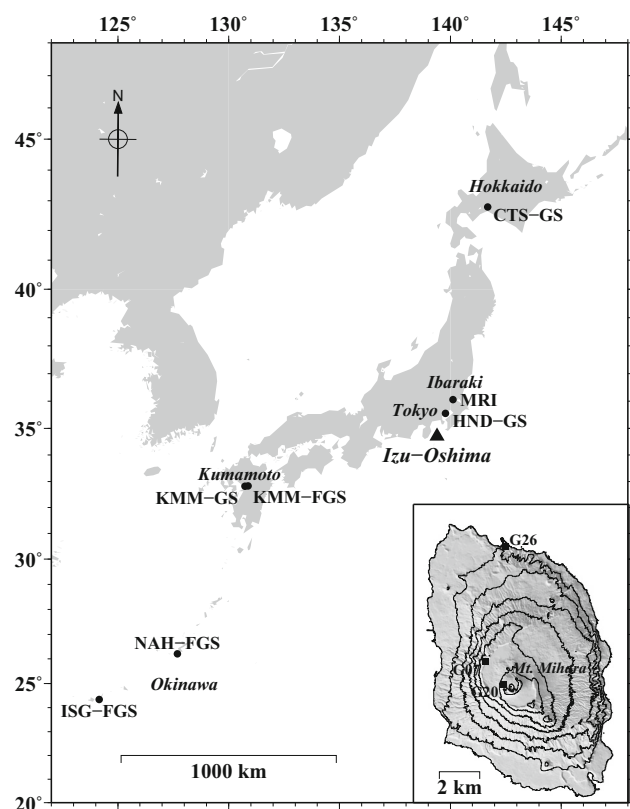 Agency, 1-1 Nagamine, Tsukuba, Ibaraki 305-0052, Japan

Fig. 1 Locations of the absolute gravity stations used for the scale factor calibration measurements. Triangle: location of the Izu-Oshima volcano. Insert map: topographic relief map of Izu-Oshima volcano. Topographic contour interval is 100 m

measurements conducted for the CG-5#033 using the JGSN stations. Then, I show the features of estimated scale factors and a way to correct them. Finally, I discuss the reason for phenomena in terms of the scale factor observed by the CG-5#033 gravimeter and apply the corrections to repeated survey data at Izu-Oshima volcano as an example.

2 Instrumental parameter settings

In order to discuss the scale factor of the CG-5 gravimeter, the most important instrumental parameters to consider are GCAL1 and GCAL2. The parameters GCAL1 and GCAL2 define the sensitivity of the CG-5 gravimeter sensor. These two factors are used to translate the A/D converter output of the feedback DC voltage normalised by the calibration voltage into a gravity reading unit (mGal):

$$g^{\text{read}} = \text{GCAL1} \times AD_{\text{out}} + \text{GCAL2} \times AD_{\text{out}}^2, \tag{1}$$

where g^{read} and AD_{out} are the gravity reading and the A/D converter output, respectively (equation B.4 in Scintrex Ltd 2010). According to Scintrex Ltd (2010), GCAL1 is set by the

manufacturer before shipping, based on calibration measurements performed in Toronto, Canada, while GCAL2, which accounts for a small quadratic nonlinearity, has been reduced to zero by an electronic adjustment.

Operations conducted using the CG-5#033 should be divided into two periods with regard to the parameter settings. The first period (Period 1) started in October 2004 and continued until 2010. During Period 1, GCAL1 was set to be 8200.007 based on a calibration dated 12 October 2004, before it was shipped by the manufacturer. In the summer of 2010, an electrical failure of the display module occurred, and the gravimeter was shipped to the manufacturer to be repaired. GCAL1 was reset to 8206.725 by the manufacturer during the repairs, on 19 October 2011. The second period (Period 2) started in October 2011 and has continued until present. The ratio between the values of GCAL1 during Period 2 and Period 1 equals 1.000819 (Table 1). This result implies that the sensitivity of the instrument changed by about 819 ppm during 7 years (from 2004 to 2011). All of the calibration measurements using the JGSN stations described below were done in Period 2.

3 Calibrations of the CG-5#033

3.1 Calibration measurements at the JGSN stations

To constrain the scale factor of the CG-5#033, calibration measurements have been conducted since 2012 using JGSN absolute gravity stations. This nationwide network was established by the Geospatial Information Authority of Japan (GSI; Geographical Survey Institute 1976; Yamaguchi et al. 1997). The latest version of the JGSN was released in 2017 as JGSN2016. The JGSN2016 includes 32 fundamental gravity stations (FGSs) and 231 first-order gravity stations (GSs). Gravity values were determined at the FGSs by absolute gravimeters, while at the GSs they were adjusted by relative measurements from the FGSs. At the FGSs, vertical gravity gradients were also observed (Yahagi et al. 2018). The nationwide network was used for the calibrations in order to minimise the effects of (1) inevitable measurement errors, (2) inaccurate correction procedures and (3) possible gravity changes at the reference gravity stations, by referring large gravity intervals.

Six calibration campaigns were conducted (A to F in Fig. 2a). All the measurements were done along a round trip, which started from and finished at the MRI in Tsukuba City (Ibaraki), about 50 km NE of Tokyo. From March 2012 until July 2017, two calibration campaigns (A and C) were for the Naha FGS (NAH-FGS, Okinawa), at lower latitude (lower gravity); the other two campaigns (B and D) were for the Chitose GS (CTS-GS, Hokkaido), at higher latitude (higher gravity), via the Haneda GS (HND-GS) in

Table 1 Parameter settings for the CG-5#033 gravimeter

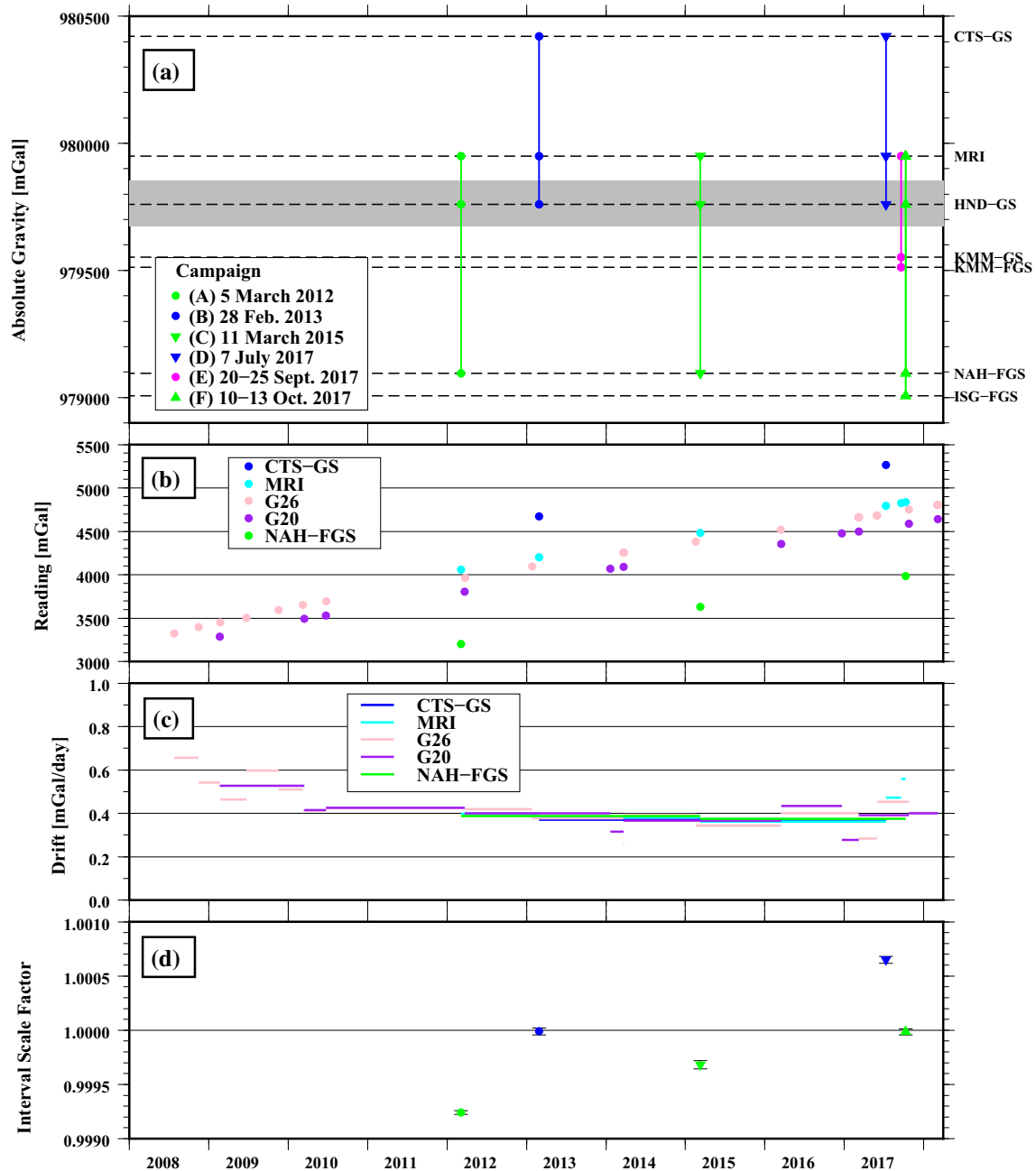| Period	Date setting	Calibration factors		Factor for adjusting to setting in Period 2
		GCAL1	GCAL2	
1	October 12, 2004	8200.007	0	1.000819
2	October 19, 2011	8206.725	0	–

Fig. 2 History of the calibration campaigns and time series of the gravity readings, instrumental drift, and scale factors. **a** History of the calibration campaigns and absolute gravity values at the stations where the measurements took place. The grey area indicates the gravity range at Izu-Oshima. **b** Gravity readings at selected stations. **c** Instrumental drifts translated from the gravity reading values shown in (**b**). **d** Interval scale factors calculated for the station combinations MRI—NAH-FGS and MRI—CTS-GS. Colours and symbols are the same as in (**a**)

Table 2 List of gravity stations used for the calibration measurements

Station	Code	Latitude (°N)	Longitude (°E)	Altitude (m)	Absolute gravity (mGal)	Vertical gradient[1] (mGal/m)
Chitose GS	CTS-GS	42.785808	141.680453	24	980421.55	0.322[2]
Haneda GS	HND-GS	35.549167	139.784167	− 2	979759.54	0.298[2]
Kumamoto FGS	KMM-FGS	32.835503	130.870972	184	979511.94	0.325
Kumamoto GS	KMM-GS	32.816914	130.727794	23	979551.64	0.325[3]
Naha FGS	NAH-FGS	26.207453	127.686811	21	979095.96	0.282
Ishigakijima FGS	ISG-FGS	24.336639	124.164656	7	979006.04	0.331
MRI	MRI	36.055639	140.125250	22	979948.92[3]	0.318[3]
Tsukuba FGS[4]	TKB-FGS	36.103919	140.086933	21	979951.22	0.294

1. Downward positive
2. After Ukawa et al. (2010)
3. Observed for this study
4. Used for tying to MRI

Tokyo. Two additional campaign measurements were conducted in September and October 2017. Campaign E was for Kumamoto (KMM-FGS and KMM-GS). Campaign F was toward the Ishigakijima FGS (ISG-FGS) to observe the lowest absolute gravity among the JGSN via the HND-GS and the NAH-FGS. The absolute gravity value at the MRI was determined by tying the Tsukuba FGS (TKB-FGS, 6 km NNW of the MRI): the difference in gravity value was − 2.30 mGal. Overall, the absolute gravity stations of the three FGSs (KMM-FGS, NAH-FGS and ISG-FGS), the three GSs (CTS-GS, HND-GS and KMM-GS) and the MRI were used for the calibration (Table 2). In addition, during campaign E, supplemental measurements at a site different from the JGSN stations were conducted to constrain the instrumental drift.

The total gravity difference between the lowest value at the ISG-FGS and the highest value at the CTS-GS is approximately 1.4 Gal. For example, gravity intervals of MRI–NAH-FGS and MRI–CTS-GS are 853 mGal and 473 mGal, respectively. Then, errors of 85 μGal and 47 μGal are allowed to achieve an accuracy of 100 ppm for the scale factor, when they are determined by translating the absolute and observed gravity differences.

The measurements were essentially based on the profile method (Torge 1989): that is, the measurements at each station were conducted during both the outward and homeward ways to constrain the instrumental drift. One exception was the KMM-FGS during the campaign E: the measurement was done during only the outward way. Designs and conditions of the measurements were different depending on the campaign. The round-trip duration was one day for campaigns A to D, to minimise the effect of changes in the drift rate. However, it was of four days and two days for campaigns E and F, respectively, due to logistic problems. To better constrain the instrumental drift during campaigns E and F, additional continuous measurements were conducted at the MRI, before

and after the respective round trips. Therefore, data of six days and three days were included in the analysis of campaign E and F, respectively. According to such conditions, at each station, from three at least to over 1000 measurements of 57–60 s were conducted during both the outward and the homeward ways (Table 3).

In the initial phase of some of the measurements, gradual increases in gravity readings were recognised. These increases probably indicate a recovery from the high tilt susceptibility pointed out by Reudink et al. (2014). Such data were manually omitted when the gravity values were observed enough time to recover. However, data from campaign C were probably affected by this problem, because few data were recorded at each station. The measurements of campaign A were conducted after 11 hours of the start of power supply and probably include some transient heating effects of the instrument. Although not obtained under ideal conditions, the data from this campaign were examined in a similar manner to those of other campaigns. Among all the stations, the HND-GS at Haneda International Airport is the noisiest, because of the heavy traffic. Therefore, for this station, the estimated relative gravity values generally include larger errors.

3.2 Gravity values at the calibration stations

Using the observed data, relative station gravity values were determined for each campaign. First, the effects of tide, atmospheric pressure and instrumental height were corrected for each reading. For the tidal corrections, the solid earth tide and ocean tidal loading effects were calculated using GOTIC2 (Matsumoto et al. 2001). The effect of the atmospheric pressure was corrected by considering an admittance of − 0.000356 mGal/hPa (Merriam 1992). Incorrect vertical gravity gradients and instrumental heights easily lead to correction errors up to several tenths of a μGal (Lederer

Table 3 Settings and results of the calibration measurements for each campaign

Calibration measurement	Station	Number of measurements	Gravity reading (mGal)	Difference[1] (mGal)	RMS[2] (mGal)
(A) 5 March 2012	MRI	86	4056.906	–	0.005
	HND-GS	7	3867.456	− 189.451	0.011
	NAH-FGS	82	3203.291	− 853.615	0.002
	Total	175			0.004
(B) 28 Feb. 2013	MRI	19	4200.013	–	0.004
	HND-GS	8	4010.554	− 189.459	0.010
	CTS-GS	17	4672.641	472.628	0.004
	Total	44			0.004
(C) 11 March 2015	MRI	6	4483.093	–	0.028
	HND-GS	8	4293.685	− 189.408	0.029
	NAH-FGS	6	3629.855	− 853.238	0.001
	Total	20			0.024
(D) 12 July 2017	MRI	50	4792.114	–	0.002
	HND-GS	26	4602.777	− 189.337	0.010
	CTS-GS	28	5264.430	472.316	0.002
	Total	104			0.006
(E) 20–25 Sept. 2017	MRI	2735	4825.122	–	0.003
	KMM-GS	130	4427.924	− 397.198	0.002
	KMM-FGS	60	4388.210	− 436.912	0.001
	(Supplemental)[3]	2412	4426.718	− 398.404	0.003
	Total	5337			0.003
(F) 10–13 Oct. 2017	MRI	624	4836.299	–	0.003
	HND-GS	36	4646.936	− 189.363	0.017
	NAH-FGS	120	3983.320	− 852.979	0.019
	ISG-FGS	320	3893.391	− 942.909	0.002
	Total	1100			0.007

1. Gravity differences referred to MRI
2. Root-mean-squares of residuals
3. Supplemental station

2009); therefore, the vertical gravity gradient observed at each station was reflected for the instrumental height correction (Table 2). The gradients for the FGSs were measured by the GSI; for the CTS-GS and the HND-GS, the gradients reported by Ukawa et al. (2010) were used instead. For the KMM-GS and the MRI, I observed gradients of 0.325 mGal/m and 0.318 mGal/m, respectively. The instrumental heights measured at the top plane of the gravimeter were reduced to the height of the sensor by subtracting 21.1 cm from the height of the former.

After applying the corrections to each reading, the relative gravity values for all stations and the instrumental drift rate were determined simultaneously. A gravity reading after the tidal, atmospheric pressure and instrumental height corrections at the i-th station and at the time t_k is described by introducing a linear drift term:

$$g_i^{\mathrm{read}}(t_k) = g_i^{\mathrm{read}} + D(t_k - t_0), \qquad (2)$$

where D and t_o are the drift rate and the time of the first reading at the first station, respectively. g_i^{read} is the final gravity reading at an i-th station after the drift correction. For I stations within a campaign, the unknown parameters $g_i^{\mathrm{read}} (i = 1, \ldots, I)$ and D were estimated by the least-squares calculation using all the readings of one round trip. Gravity reading deviations were calculated as the root-mean-squares (RMS) of the residuals. The final gravity readings and the RMS are summarised in Table 3.

Nonlinear drifts are a concern, particularly in the longer campaigns of E and F. However, behaviours are not simple. For example, for the longest campaign (E, of six days), the linear drift fitted well and the residual RMS of all its stations were lower than 0.003 mGal after the linear drift fitting. On the contrary, the three-day campaign F included fluctuations (perhaps due to long-lived high tilt susceptibility and inaccurate tidal corrections for the NAH-FGS, the ISG-FGS at isolated islands). Although such fluctuations can be fitted

using nonlinear drift models with higher order polynomials, it is difficult to judge whether such procedures are physically meaningful. Therefore, I adopted the linear drift model so as that the deviations from this model are expressed as larger residual RMS.

Data from campaigns B and D, toward the CTS-GS, are of relatively good quality: the RMS are less than 0.004 mGal, except for the noisiest station (HND-GS). On the other hand, large residual RMS for the data collected during campaign C suggest the presence of errors linked to high tilt susceptibility. A negative drift was observed for campaign A, which started after 11 hours from the beginning of the power supply; however, the linear drift fitting worked well for the corresponding round trip.

3.3 Long-term instrumental drift

Before the estimation of the scale factor, the long-term instrumental drift of the CG-5#033 gravimeter should be mentioned: this drift played an important role in this study. The history of CG-5#033 gravity readings at selected stations is plotted in Fig. 2b. Here are plotted the JGSN stations, accompanied by stations G20 and G26 located on the Izu-Oshima volcano (Fig. 1, characterised by high measurement frequencies). The GCAL1 for Izu-Oshima data during Period 1 is adjusted to that of Period 2 multiplying the factor by 1.000819 (Table 1). Monotonic increases in gravity readings indicate the occurrence of continuous instrumental drifts. The long-term instrumental drifts between measurements can be estimated from the gravity readings series (Fig. 2c). As seen in the figure, the CG-5#033 gravimeter experienced a long-term instrumental drift of the order of 0.1 mGal/day. (It seems to decrease gradually from ca. 0.4–0.7 mGal/day during Period 1 to ca. 0.3–0.6 mGal/day during Period 2.)

3.4 Scale factor estimation

In the following section, I estimate the scale factor by comparing the gravity values measured by the CG-5#033 gravimeter (Table 3) with the known absolute gravity values (Table 2).

3.4.1 Interval scale factor

First, the scale factor is estimated for each gravity interval. Hereafter, this is called as an interval scale factor. The interval scale factor S_{ij}^{int} for a gravity difference of i-th and j-th stations is calculated based on the following equation:

$$\Delta g_{ij}^{\text{abs}} = S_{ij}^{\text{int}} \Delta g_{ij}^{\text{read}}, \tag{3}$$

where $\Delta g_{ij}^{\text{abs}}$ and $\Delta g_{ij}^{\text{read}}$ are the differences between the known absolute gravity values and between the gravity values measured by the CG-5#033 gravimeter, respectively. The error of the estimated interval scale factor $\epsilon_{ij}^{\text{int}}$ depends on the errors of both the absolute gravity stations ϵ_i^{abs}, ϵ_j^{abs} and of the gravity readings measured by the CG-5#033 gravimeter ϵ_i^{read}, ϵ_j^{read}:

$$\epsilon_{ij}^{\text{int}} = |S_{ij}^{\text{int}}|\sqrt{(\epsilon_{ij}^{\text{abs}}/\Delta g_{ij}^{\text{abs}})^2 + (\epsilon_{ij}^{\text{read}}/\Delta g_{ij}^{\text{read}})^2}, \tag{4}$$

where

$$\epsilon_{ij}^{\text{abs}} = \sqrt{\epsilon_i^{\text{abs}^2} + \epsilon_j^{\text{abs}^2}} \tag{5}$$

$$\epsilon_{ij}^{\text{read}} = \sqrt{\epsilon_i^{\text{read}^2} + \epsilon_j^{\text{read}^2}}. \tag{6}$$

The error of each absolute gravity is assumed to be 10 μGal, so as to be the error of the absolute gravity difference is 14 μGal. For the error of each gravity reading, RMS of residuals after the calibration measurements are used.

The time series of the interval scale factors for selected station combinations (MRI–NAH-FGS, MRI–CTS-GS) are plotted in Fig. 2d. For both the station combinations, the estimated scale factor clearly increased with time. However, it seems that there is an offset of the increasing trends between both the combinations.

Figure 3a shows the estimated interval scale factors for all possible station combinations and all calibration campaigns. The factors varied between 0.9991 and 1.0006. Such a difference of 1500 ppm should be corrected for microgravity surveys. However, a systematic pattern for the scale factors could not be recognised based on these plots.

The interval scale factors for the gravity reading ranges of the CG-5#033 gravimeter are plotted in Fig. 3b, instead of the gravity differences. The endpoints of the horizontal bars indicate the gravity readings at the two stations used for the interval scale factor estimation. A positive correlation can be observed between the estimated scale factors and the gravity reading ranges. The estimated scale factors vary between 0.9991 at 3500 mGal, to 1.0006 at 5000 mGal. Several data points deviate from this trend. This is primarily due to the use of extremely small gravity differences in the estimation of the interval scale factor, following the formula shown in Eq. (4) (see the range of small gravity differences in Fig. 3a). Therefore, the interval scale factors of the estimated errors greater than 100 ppm are omitted in Fig. 3c, in order to render more clearly the general trend.

Because of the instrumental drift mentioned above, the range of gravity readings shifted with time even though the measurements are conducted at the same station combinations. Further, gravity reading ranges can overlap even though the measurements were conducted in different absolute grav-
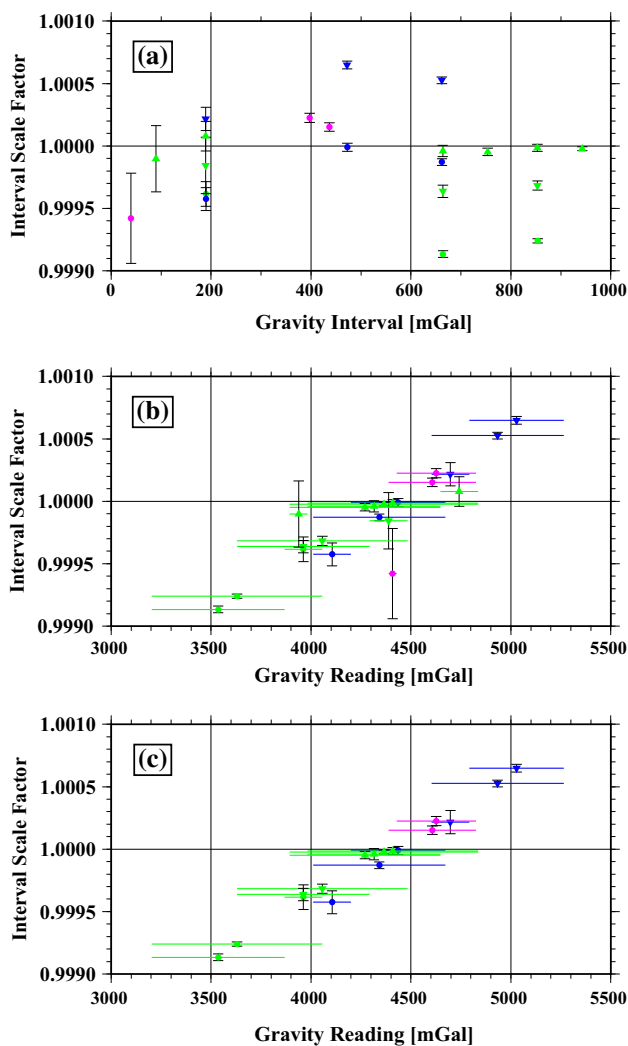
Fig. 3 Interval scale factors. Colours and symbols are the same as in Fig. 2a. **a** Plot for the gravity intervals. **b** Plot for the gravity readings of the CG-5#033. **c** Same as in (**b**), but the interval scale factors of the estimated errors greater than 100 ppm are omitted

ity ranges. However, it should be noted that for similar gravity reading ranges, the estimated interval scale factors were not significantly different, even though they were measured at different station combinations and times. This indicates that the scale factor of the CG-5#033 gravimeter primarily depends on the gravity reading ranges, regardless of the absolute gravity ranges and observation times.

3.4.2 Reading-dependent scale factor

Since it became clear that the scale factor primarily depends on the gravity readings, a formula to perform scale corrections could be created. By introducing a gravity reading-dependent scale factor $S(g_i^{\text{read}})$ in an L-th order polynomial expression as

$$S(g_i^{\text{read}}) = \sum_{l=0}^{L} c_l g_i^{\text{read}\,l}, \tag{7}$$

the scale-corrected gravity reading g_i^{corr} can be written as

$$g_i^{\text{corr}} = S(g_i^{\text{read}}) g_i^{\text{read}} = \sum_{l=0}^{L} c_l g_i^{\text{read}\,l+1}, \tag{8}$$

where c_l and g_i^{read} are the coefficients of an l-th order and the gravity reading at an i-th station before the correction, respectively. Therefore, the observation equation for the i-th and j-th station combination can be written as

$$\Delta g_{ij}^{\text{abs}} = \Delta g_{ij}^{\text{corr}} \tag{9}$$

$$= S(g_j^{\text{read}}) g_j^{\text{read}} - S(g_i^{\text{read}}) g_i^{\text{read}} \tag{10}$$

$$= \sum_{l=0}^{L} c_l (g_j^{\text{read}\,l+1} - g_i^{\text{read}\,l+1}), \tag{11}$$

where $\Delta g_{ij}^{\text{abs}}$ and $\Delta g_{ij}^{\text{corr}}$ are the gravity differences in the absolute gravity stations and the scale-corrected readings, respectively. The unknown parameters c_ls can be solved by applying the least-squares method, using the gravity differences of the possible station combinations.

Each equation is weighted by the inverse of an error ϵ_{ij} as follows:

$$\epsilon_{ij} = \sqrt{\epsilon_{ij}^{\text{abs}2} + \epsilon_{ij}^{\text{corr}2}}, \tag{12}$$

where $\epsilon_{ij}^{\text{abs}}$ and $\epsilon_{ij}^{\text{corr}}$ are errors of the absolute gravity difference and of the difference of scale-corrected gravity readings, respectively. $\epsilon_{ij}^{\text{corr}}$ is expressed as

$$\epsilon_{ij}^{\text{corr}} = \sqrt{\epsilon_i^{\text{corr}2} + \epsilon_j^{\text{corr}2}}. \tag{13}$$

The relationship between ϵ_i^{corr} and ϵ_i^{read} is expressed by differentiating Eq. (8):

$$\epsilon_i^{\text{corr}} = \sum_{l}^{L} (l+1) c_l g_i^{\text{read}\,l} \epsilon_i^{\text{read}}. \tag{14}$$

By assuming that the scale factor has a value close to 1 (that is, $c_0 \sim 1$ and $c_l g_i^{\text{read}\,l} \ll 1 (l = 1, \ldots, L)$),

$$\epsilon_i^{\text{corr}} \sim \epsilon_i^{\text{read}}. \tag{15}$$

Therefore, Eq. (12) can be written as

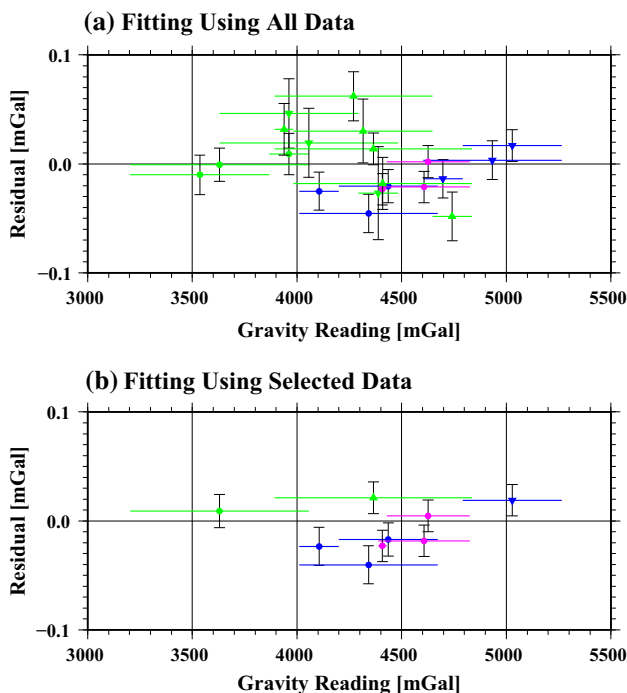$$\epsilon_{ij} \sim \sqrt{\epsilon_{ij}^{\text{abs}2} + \epsilon_{ij}^{\text{read}2}}, \tag{16}$$

(a) Fitting Using All Data

(b) Fitting Using Selected Data

Fig. 4 Residuals of calibration measurement data after the first-order reading-dependent scale factor fittings. Colours and symbols are the same as in Fig. 2a. **a** Plot for the whole dataset. **b** Plot for the same dataset, but using selected data

where $\epsilon_{ij}^{\text{abs}}$ and $\epsilon_{ij}^{\text{read}}$ are expressed as in Eqs. (5) and (6), respectively.

Two datasets of gravity differences were examined to determine the coefficients of the reading-dependent scale factor. The first dataset consisted of 21 gravity differences, from all station combinations of all campaigns, without any data screening. The second dataset consisted of nine gravity differences; in this case, the residual RMS of two stations were less than $10\,\mu$Gal. The best fit parameters (c_0, c_1) for both datasets, considering a first-order polynomial, are summarised in Table 4. Similar parameters ($c_0 \sim 0.9956$, $c_1 \sim 4.9 \times 10^{-7}$) were obtained for both datasets. The value of c_1 is substantially large, causing a scale factor difference by the order of 1000 mGal of the gravity reading difference.

The residuals obtained after the fittings are shown in Fig. 4a, b. Since the data of the first dataset were not screened, several incorrect data were included: the residuals after the fitting were largely deviated, particularly those of campaigns C and F. In the second dataset, the residuals were less scattered. Second- and higher-order polynomials were also tested. However, as expected from the randomly deviated residuals after the first-order fittings (Fig. 4), prominent reductions in the RMS were observed for both the datasets. Therefore, the investigation was not carried on in that direction.

4 Discussion

4.1 Instrumental drift and apparent calibration shift

In the former analyses, the scale factor was expressed as depending only on gravity readings, and not on time. However, calibration shifts were recognised in the calibration campaign data (Fig. 2d). At a first glance, these results seem to be contradictory. The key to understand these phenomena is considering that the instrumental drift occurred in the CG-5#033 gravimeter.

According to Scintrex Ltd (2010), the drift of the CG-5 sensor is caused by an unavoidable creep of the quartz spring, whose length under tension increases, on the average, by 0.5 ppm/day at the operating temperature of 60 °C. The CG-5#033 gravimeter in particular experienced a long-term instrumental drift of 0.3–0.7 mGal/day (Fig. 2c). Such a drift rate is sufficiently large to cause an apparent calibration shift in repetitive measurements at fixed gravity ranges, by combining the reading-dependent scale factor described above.

From Eq. (7), the first-order reading-dependent scale factor is described as:

$$S(g_i^{\text{read}}) = c_0 + c_1 g_i^{\text{read}}. \tag{17}$$

Thus, for the gravity readings at a specified station, a rough estimate of a yearly calibration shift can be made by assuming the 4.9×10^{-7}/mGal of the reading-dependent scale factor and 0.45 mGal/day of the drift rate as:

Yearly Calibration Shift
$$\sim 4.9 \times 10^{-7}/\text{mGal} \times 0.45\,\text{mGal/day} \times 365\,\text{day}$$
$$\sim 8.0 \times 10^{-5}/\text{year}.$$

Hence, a calibration shift of 800 ppm can be expected after 10 years.

Note that the expression of the interval scale factors for the gravity differences between stations is different from Eq. (17). The first-order reading-dependent interval scale factor can be expressed by using Eqs. (3) and (9) to (11) as:

$$S_{ij}^{\text{int}} = \frac{c_o(g_j^{\text{read}} - g_i^{\text{read}}) + c_1(g_j^{\text{read}\,2} - g_i^{\text{read}\,2})}{g_j^{\text{read}} - g_i^{\text{read}}} \tag{18}$$

$$= c_0 + c_1(g_i^{\text{read}} + g_j^{\text{read}}). \tag{19}$$

In case that the gravity difference is much smaller than the gravity readings (that is, $g_i^{\text{read}} \sim g_j^{\text{read}}$), the interval scale factor becomes

$$S_{ij}^{\text{int}} \sim c_0 + 2c_1 g_i^{\text{read}}, \tag{20}$$

Table 4 Coefficients of the first-order reading-dependent scale factor, RMS after the fitting and the corrected calibration factors

Dataset	Coefficients of reading-dependent scale factor				RMS (mGal)	Calibration factors	
	c_0		c_1			GCAL1$'$	GCAL2$'$
All	0.9956799968	(0.0000708204)	0.0000004906	(0.0000000083)	0.024	8171.272	33.039
Selected	0.9956492001	(0.0000919565)	0.0000004932	(0.0000000107)	0.021	8171.019	33.217

The values given in parentheses are the standard deviations of the estimated coefficients

so as that the calibration shift is twice of one for gravity readings.

In summary, the calibration shifts recognised in repeated measurements at fixed gravity ranges are apparently caused by (1) the scale factor dependence on gravity reading ranges and (2) the shift of the gravity reading ranges due to the instrumental drift.

4.2 Possible explanation for symptoms of the CG-5#033 scale factor

Scintrex Ltd (2010) described that the scale calibration of the CG-5 gravimeter is expressed as Eq. (1). They documented the possible causes for changes in the calibration factor GCAL1. The stability of GCAL1 depends on (1) the dimensional stability of the capacitive displacement transducer, (2) the stability of the internal DC reference voltage, (3) the stress relaxation effects on the newly fused quartz, causing changes in GCAL1 during an initial period of a few months. Still, the shift of the calibration factor is not prominent in the CG-5#033 gravimeter. In fact, the scale factor is stable, regardless of the gravity range observation time (Fig. 3c); moreover, the calibration shift is caused by the instrumental drift.

One way to explain the phenomena occurred in the CG-5#033 scale factor is to consider the existence of a nonlinear relationship between the A/D converter output and the gravity reading, when the symptoms within concepts written in the user manual are considered. Although Scintrex Ltd (2010) reported that the nonlinearity is reduced to zero by an electronic adjustment and that GCAL2 is set to be zero, the reading-dependent scale factor still suggests that the nonlinear term is not trivial. The scale-corrected reading is described by inserting Eq. (1) into Eq. (8):

$$g^{\text{corr}} = S(g^{\text{read}})(\text{GCAL1} \times AD_{\text{out}} + \text{GCAL2} \times AD_{\text{out}}^2). \quad (21)$$

Since GCAL2 is set to be zero, Eq. (21) becomes:

$$g^{\text{corr}} = \sum_{k=0}^{1} c_k (\text{GCAL1} \times AD_{\text{out}})^{k+1} \quad (22)$$

$$= \text{GCAL1}' \times AD_{\text{out}} + \text{GCAL2}' \times AD_{\text{out}}^2 \quad (23)$$

where

$$\text{GCAL1}' = c_0 \text{GCAL1}$$
$$\text{GCAL2}' = c_1 \text{GCAL1}^2,$$

if the first-order polynomial expression is adopted as the reading-dependent scale factor. The corrected calibration factors GCAL1$'$ and GCAL2$'$ for the c_0 and c_1 of the two datasets are listed in Table 4. If further higher-order forms for the reading-dependent scale factor are adopted,

$$\text{GCAL3}' = c_2 \text{GCAL1}^3$$
$$\text{GCAL4}' = c_3 \text{GCAL1}^4$$

and so on. Although it is not possible to affirm yet whether the nonlinear relationship between the A/D output and the gravity readings is the cause of the phenomena, the functional form of the higher-order polynomial expression explains well the symptoms of the CG-5#033.

4.3 Correction of Izu-Oshima data

The new reading-dependent scale factor is applied to the repeated survey data of Izu-Oshima volcano to show the effect of the scale corrections. Since the coefficients c_0 and c_1 determined by both the datasets using all the data and the selected data are similar (Table 4), time series of the corrected gravity values are almost identical. Therefore, only the corrections using the selected data are shown below.

Figure 5a shows the time series of the gravity readings of the CG-5#033 for selected stations in Izu-Oshima. As described in Sect. 3.3, the gravity readings increase with the passage of time due to the instrumental drift. The scale factor for each reading shown in Fig. 5a can be calculated by applying Eq. (17) and the coefficients c_0 and c_1 (Fig. 5b). The estimated scale factors increase from ca. 0.9973 in 2008–2009 to ca. 0.9980 in 2017–2018. About 700 ppm of the apparent calibration shift occurred as the rough estimate described in Sect. 4.1.

Two examples for selected station combinations are shown. Time series of the interval scale factors calculated by Eq. (19) and gravity differences before and after the scale correction are shown in Fig. 5c–f. The first example (Fig. 5c–d) is gravity values of G20 at the summit area relative to G26
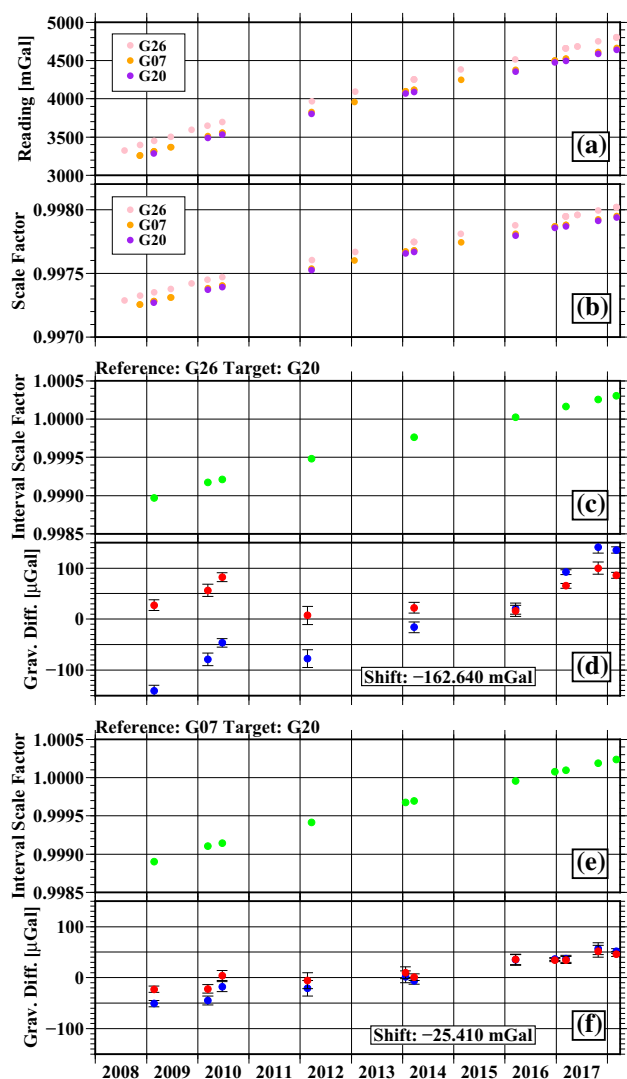
Fig. 5 Time series of the gravity readings and the scale factors for selected station, the interval scale factor and gravity differences for selected station combinations of the repeated microgravity survey at Izu-Oshima volcano. **a** Gravity readings for the selected stations G26, G07 and G20. **b** Scale factors for the gravity readings shown in (**a**). **c** and **d** Interval scale factors (**c**) and gravity differences (**d**) for the station combination G26 and G20. **e** and **f** Interval scale factors (**e**) and gravity differences (**f**) for the station combination G07 and G20. Blue and red circles in (**d**) and (**f**) indicate gravity differences before and after the scale factor corrections, respectively

at the northern coastal area, having − 163 mGal of a gravity difference. This combination intends to monitor island scale gravity changes. The second example (Fig. 5e, f) is gravity values of G20 relative to G07 at the northwestern caldera rim to monitor local gravity changes of the central cone Mt. Mihara. The gravity difference is − 25 mGal. In both the cases, the apparent calibration shifts are clearly recognised (Fig. 5c, e). Note that values of the interval scale factors and the magnitude of the calibration shifts are different from those of the scale factors for the gravity readings (Fig. 5b) as men-

tioned in Sect. 4.1. The interval scale factor increases from 0.9989–0.9990 in 2009 to 1.0002–1.0003 in 2018. That is, ca. 1300 ppm of the calibration shift occurred during 9 years. Before the scale corrections, monotonic increases in the gravity differences are recognised in the both cases (blue circles in Fig. 5d, f: about 300 μGal and 100 μGal during 9 years for the first and second examples, respectively.). Such increases are suppressed by applying the scale corrections (red circles in Fig. 5d, f). After the corrections, about 100 μGal of a fluctuation is recognised in the first example (Fig. 5d). This probably reflects an infiltration of meteoric water into the volcanic edifice due to precipitations. In the second example, 70 μGal of gravity increase during 9 years remains (Fig. 5f). The primary cause of the gradual increase is probably a free-air effect because a continuous subsidence localised at Mt. Mihara has been observed. For quantitative investigation of such physical processes under the volcano, the scale corrections are essential. The gravity changes at Izu-Oshima volcano described above will be discussed in future papers.

4.4 Suggestions for future calibration measurements

The scale factor for the CG-5#033 gravimeter, expressed by the reading-dependent form, should be continuously updated. The scale factor in the present work was obtained considering gravity readings comprised between 3200 and 5300 mGal. However, the reading ranges for specific regions, like the Izu-Oshima, will be beyond the calibration range in future, because of the 0.3–0.7 mGal/day instrumental drift. Future calibration measurements should be done considering higher gravity ranges (i.e., higher latitudes), to construct a new reading-dependent scale factor including higher gravity reading ranges.

5 Summary and conclusions

The scale calibration measurements for the CG-5#033 gravimeter were conducted using the nationwide absolute gravity network. The following characteristics were recognised:

1. The scale factor of the CG-5#033 gravimeter depends primarily on the gravity reading ranges: for similar gravity reading ranges, no significant differences in the estimated scale factors were recognised, even though the data were obtained at different station combinations and different times. Therefore, the gravity readings can be corrected by introducing a gravity reading-dependent scale factor.
2. Calibration shifts were recognised during repeated calibration measurements on the same station combinations; this happened although the scale factor essentially

depends on gravity readings, not on time. This phenomenon can be explained by considering the long-term instrumental drift of the CG-5 gravimeter. The calibration shifts recognised during the repeated measurements were apparently caused by (1) the scale factor dependence on the gravity reading ranges and (2) the shift of the gravity reading ranges due to the instrumental drift.

References

Biegert E, Ferguson J, Li X (2008) 4D gravity monitoring—introduction. Geophysics 73:WA1–WA2

Budetta G, Carbone D (1997) Potential application of the Scintrex CG-3M gravimeter for monitoring volcanic activity: results of field trials on Mt. Etna, Sicily. J Volcanol Geotherm Res 76:199–214

Carbone D, Rymer H (1999) Calibration shifts in a LaCoste-and-Romberg gravimeter: comparison with a Scintrex CG-3M. Geophys Prospect 47:73–83

Geographical Survey Institute (1976) Establishment of the Japan Gravity Standardization Net 1975. J Geod Soc Jpn 22:65–76

Lederer M (2009) Accuracy of the relative gravity measurement. Acta Geodyn Geomater 6:383–390

Matsumoto K, Sato T, Takanezawa T, Ooe M (2001) GOTIC2: a program for computation of oceanic tidal loading effect. J Geod Soc Jpn 47:243–248

Merriam JP (1992) Atmospheric pressure and gravity. Geophys J Int 109:488–500

Meurers B (2018) Scintrex CG5 used for superconducting gravimeter calibration. Geod Geodyn 9:197–203

Parseliunas E, Petroskevicius P, Birvydiene R, Obuchovski R (2011) Investigation of the automatic gravimeters Scintrex CG-5 and analysis of gravimetric measurements. In: Selected papers, 8th international conference on environment engineering, May 19–20, 2011. Vilnius, Lithuania 2011, pp 1416–1423

Reudink R, Klees R, Francis O, Kusche J, Schlesinger R, Shabanloui A, Sneeuw N, Timmen L (2014) High tilt susceptibility of the Scintrex CG-5 relative gravimeters. J Geod 88:617–622

Scintrex Ltd (2010) CG-5 Scintrex autograv system operation manual, part # 867700 Revision 7. Scintrex Limited, Concord

Torge W (1989) Gravimetry. Walter de Gruyter, Berlin, p 465

Ukawa M, Nozaki K, Ueda H, Fujita E (2010) Calibration shifts in Scintrex CG-3M gravimeters with an application to detection of microgravity changes at Iwo-tou caldera, Japan. Geophys Prospect 58:1123–1132

Williams-Jones G, Rymer H, Mauri G, Gottsmann J, Poland M, Carbone D (2008) Toward continuous 4D microgravity monitoring of volcanoes. Geophysics 73:WA19–WA28

Yahagi T, Yoshida K, Miyazaki T, Hiraoka Y, Miyahara B (2018) Establishment of the Japan Gravity Standardization Net 2016 (JGSN2016). J Geod Soc Jpn 64:14–25

Yamaguchi K, Nitta K, Yamamoto H, Matsuo K, Machida M, Murakami M, Ishihara M, Nakai S, Shichi R, Yamamoto A (1997) The establishment of the Japan Gravity Standardization net 1996. Gra-GeoMar96. Proc Int Symp 117:241–248